Akademie věd
České republiky

Teze disertace
k získání vědeckého titulu "doktor věd"
ve skupině věd **chemických**

Proton-Electron Transfer Reactivity of Enzymatic and Biomimetic Transition Metal Complexes

Komise pro obhajoby doktorských disertací v oboru **fyzikální chemie**

Uchazeč: **Martin Srnec**

Pracoviště: **Ústav fyzikální chemie J. Heyrovského, AV ČR**

Místo a datum: **Praha, 30. listopad 2023**

Summary

Here, I present my major scientific achivements in the field of chemical reactivity, which includes (*i*) my contributions to elucidation of key reactive intermediates in several catalytic pahways of non-heme iron (NHFe) enzymes and the relevation of their electronic-structure properties and their effects on catalytic efficiency, and (*ii*) the methodological and conceptual works on H-atom abstraction reactions, which are placed at core of many important (bio)chemical transformations and (bio)energetic processes catalyzed among others by NHFe enzymes.

The presented topics follow my scientific pathway along which I mostly pursued various aspects of concerted electron-proton transfer (CEPT) reactivity. Such a pathway started during my PhD studies when I mastered and employed QM/MM modeling and advanced ab initio quantum methods to explore reaction mechanisms and redox properties of several redox-active metalloproteins including Δ^9 desaturase (presented in section 3). In order to expand my expertise in redox-active enzymatic catalysis, I joined the group of Prof. Edward I. Solomon at Stanford University as a postdoc. There, during the period of two years, I mastered nuclear resonance vibrational spectroscopy and magnetic circular dichroism spectroscopy that I combined with advanced multireference quantum-chemical methods to get insight into geometric and electronic structures of the active sites of some archetypal $NHFe^{IV}O$ enzymes and their synthetic models. As a result, I elucidated a new reactive (so-called) π channel for C-H bond activation that appeared active in halogenase to control chlorination over hydroxylation, the latter of which is otherwise thermodynamically favored. This is presented in section 2. In section 3, I present electronic and catalytic properties of binuclear metal complexes, including binuclear non-heme iron ($NHFe_2$) active sites. Because all catalysts I studied involve C-H bond activation as a key step along their catalytic pathway, I naturally expanded my interest to the field of computational electrochemistry that I began to explore more deeply after my return to the Czech Republic in early 2014. While building my independent career with a small team of postdocs and PhD students, I devised a robust theoretical implicit solvation-based approach for calculating the reduction potential of a charged complex based on one or several thermodynamic cycles that involve H-atom addition/abstraction to/from an anionic/cationic species, respectively (section 4.1). This methodological work allowed me to fully realize that H-atom transfer is in fact composed of two concerted proton and electron transfers, and that the degree of their concertedness, as encoded in reduction potentials and acidity constants of the H-atom donor and acceptor, defines a new phenomenon that I named asynchronicity (section 4.2). I also found that asynchronicity can have an important effect on the reaction barrier. I recently described asynchronicity and its relation to reactivity in a PNAS article. In addition, I discovered frustration – another important and competing thermodynamic factor affecting C-H bond activation reactivity (section 4.3). In parallel, I developed a novel concept for studying chemical reactivity/selectivity in processes

including some CEPT reactions that exhibit a non-equilibrium behavior, where the classical transition state theory breaks down (section 4.4).

1. Introduction

The dissertation consists of two interconnected parts (sections 2-3 and section 4) centered around one theme - the concerted electron-proton transfer (CEPT) reactivity. The core of the first part is enzymatic catalysis, elucidation of geometric and electronic structures of the key reactive intermediates responsible for C-H bond activation. The second part is more general and methodological, dealing with the development of new concepts in chemical reactivity with the focus on CEPT reactions.

CEPT reactions are extremely important for their ubiquity and indispensability in a multitude of enzymes capable of selective homolysis of strong C−H bonds, through which plethora of substrate transformations are initiated.[1] For example, this includes heme and non-heme iron enzymes, which are essential for biosynthetic pathways of antibiotics, collagen, for DNA repair, bioremedation and synthesis of many other natural products such as neurotransmitters.[2] Many of iron enzymes form the reactive ferryl ($Fe^{IV}O$) unit in their active sites (**Scheme 1**). This unit is a powerful oxidant that can easily abstract an aliphatic hydrogen atom from various substrates, which opens the post-CEPT pathways for substrate hydroxylation, halogenation, desaturation, or ring closure.[3] However, **Scheme 1** represents only one of enzymatic strategies for C-H bond activation adopted in Nature. For example, enzymes containing two iron centers in the active site also employ various oxygenated intermediates responsible for H-atom abstraction (HAA) from substrates.[4] Despite their high reactivity, ferryl and other HAA-reactive intermediates are also fascinating for their common chemo-, site/regio- and/or stereo-selectivity. Understanding the key geometric and electronic structure properties of such intermediates and their contributions to HAA reactivity is therefore highly important for the development of the bioinspired HAA catalysis.

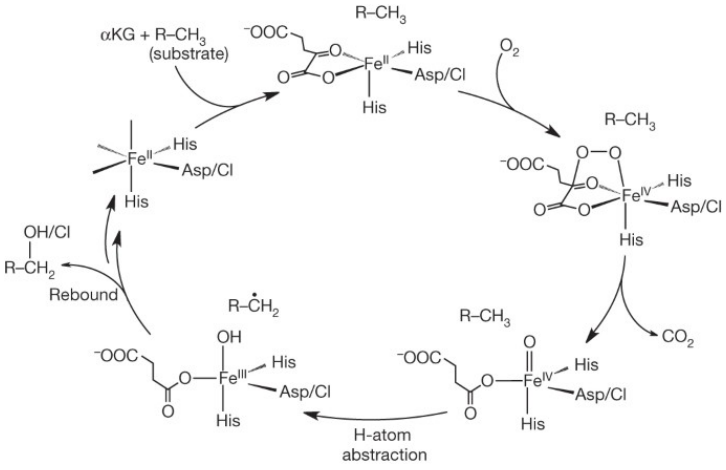

Scheme 1: The catalytic cycle of mononuclear non-heme iron hydroxylases/halogenases. Scheme taken from Ref. 5.

In sections 2-3, I present eleven theoretical and combined theoretical/experimental studies on several mononuclear and binuclear non-heme iron enzymes, complemented by studies of their biomimetic model(s). First, I introduce and comment my study on structurally well-defined (TMG_3tren)$Fe^{IV}O$ complex, which provided an unprecedented insight into the ground and excited states of the high-spin $Fe^{IV}O$ unit and reveal a novel reactive channel for H-atom abstraction pathway. This is followed by studies on geometric and electronic structure contributions to CEPT reactivity of the high-spin $Fe^{IV}O$ active site of two prototypical non-heme iron enzymes, taurine dioxygenase (TauD) and syringomycin halogenase (SyrB2). I also present our computational works leading eventually to definition of a viable HAA-reactive intermediate of one binuclear non-heme iron enzyme – Δ^9 desaturase (Δ^9D). The Δ^9D also motivated me and my collaborators to get a deeper insight into the electronic-structure complexity of binuclear transition metal complexes, leading to a formulation a novel analysis for exchange interactions between magnetic (metal) centers.

The paramount role of HAA reactions in (bio)chemistry has inspired numerous theoretical/experimental efforts to unveil the physical underpinnings of the process and their influence on reaction rates,[6,7,8] and to distinguish the mechanistic nuances of HAA.[9,10,11] Despite these advances, the design of synthetic methodologies leveraging selective HAA remains a heuristic process,[12,13] and theory is usually invoked *aposteriori* to rationalize experimental outcomes.[14,15] With the aim to fill the gap between theory and synthetic trial-and-error efforts, I started with my team to develop the new chemical concepts, the current status of which is described in the second part of the dissertation.

Thus, in section 4, I will introduce our contribution to computational electrochemistry and present how this interest evolved into the formulation of the concept of asynchronicity and frustration, which appear to be important thermodynamic (and yet overlooked) contributions to CEPT reactivity. Finally, I will also present our pioneering work on the analysis of kinetic energy distribution within the transition-state reactive mode and its applicability to CEPT reactivity and post-CEPT reaction selectivity that cannot be described by standard Eyring's transition state theory.

2. Geometric and Electronic Structure Contributions to H-atom Abstraction Reactivity

2.1 Fe^{IV}=O Model System: Interplay between Spectroscopy and Calculations and the Definition of New Reactive H-atom Abstraction Channels.

- ***Srnec M.**, Wong S. D., England J., Que Jr. L., Solomon E. I.: π-Frontier Molecular Orbitals in S=2 Ferryl Species and Elucidation of Their Contributions to Reactivity.* ***Proc. Natl. Acad. Sci. U.S.A.*** *2012, 109, 14326-14331.*
- ***Srnec M.**, Wong S. D., Solomon E. I.: Excited state potential energy surfaces and their interactions in Fe^{IV}O active sites.* ***Dalton Trans.*** *2014, 43, 17567-17577.*

Most of the synthetic Fe^{IV}O models were prepared in the *S*=1 ground state, which contrasts to the *S*=2 ground state of the enzymatic Fe^{IV}O species.[1,16] For the first structurally characterized *S*=2 Fe^{IV}O model, $(TMG_3tren)Fe^{IV}$=O,[17] we investigated electronic structure properties using the low-temperature magnetic circular dichroism (LT MCD) spectroscopy combined with the multireference calculations. From these MCD-calibrated analyses, we revealed the nature of the frontier molecular orbitals *S*=2 Fe^{IV}=O species that provide fundamental mechanistic insight into their reactivities (**Fig. 2.1-1**). We showed that the lowest-energy electronic states (and associated frontier molecular orbitals) evolve along the respective Fe–O potential energy surfaces giving rise to oxyl–Fe^{III} character at Fe–O distances, relevant to the transition state (TS) for H-atom abstraction from a substrate. For these Fe–O distances, the biologically relevant *S*=2 Fe^{IV}=O species can generate a hole in the oxo-based $p_{x,y}$ or p_z orbitals (**Fig. 2.1-1**). Thus, dπ* and dσ* frontier molecular orbitals, respectively, can be active in H-atom abstraction (one σ and two π HAA-reactive channels), providing flexibility to an Fe^{IV}O active site in controlling reaction selectivity. This contrasts to frontier molecular orbitals of the *S*=1 Fe^{IV}=O system, in which a hole is generated only in the oxo-based $p_{x,y}$ orbitals (*ie.*, π molecular orbitals) and thus, due to spin polarization, the dπ* orbitals become reactive towards H-atom abstraction. This defines the (only available) π channel for H-atom abstraction in these *S*=1 systems (that can be hindered by equatorial chelate sterics in models).

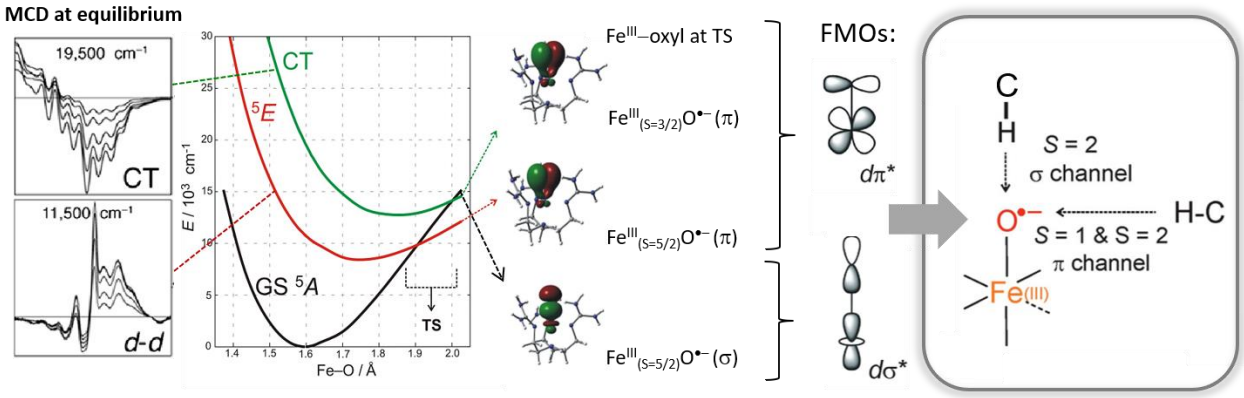

Figure 2.1-1: Correlation of the caclulations with the spectroscopic data allows to inspect an evolution of the ground and lowest excited-state wavefunctions along the Fe—O stretching mode, which leads to a definition of frontier molecular orbitals responsible for the attack of C−H bond in the either the σ- or π-

channel mode. Both of the σ and π channels are accessible for *S*=2, which contrasts to the *S*=1 space, typical for most of ferryl biomimetics. Figure adopted from Refs. 18 and 19.

2.2 The Fe^{IV}=O Active Site in Taurine Dioxygenase: Spectroscopy and Calculations and the Definition of its Geometric Structure.

- ***Srnec M.**, Iyer S. R., Dassama L. M. K., Park K., Wong S. D., Sutherlin K. D., Yoda Y., Kobayashi Y., Kurokuzu M., Saito M., Seto M., Krebs C., Bollinger Jr J. M., Solomon E. I.: Nuclear Resonance Vibrational Spectroscopy Definition of the Facial Triad FeIV=O Intermediate in Taurine Dioxygenase: Evaluation of Structural Contributions to Hydrogen Atom Abstraction. **J. Am. Chem. Soc.** 2020, 142, 18886-18896.*

The first enzymatic $Fe^{IV}O$ intermediate was trapped and spectroscopically characterized for taurine dioxygenase in 2003-2004 in the group of Bollinger and Krebs.[20] However, the determination of the geometric structure of (TauD)$Fe^{IV}O$ remained for a long time elusive. To define the structure of the $Fe^{IV}O$ active site, we combined nuclear resonance vibrational spectroscopy (NRVS) and density functional theory (DFT) calculations (**Fig. 2.2-2A** and **2.2-2B**, respectively). We showed that the (TauD)$Fe^{IV}O$ active site has a trigonal bipyramidal geometry as depicted in **Fig. 2.2-2C**. Built on this finding, we computationally probed HAA reactivity of six models that are trigonal bipyramidal, square pyramidal, and distorted octahedral $Fe^{IV}O$ complexes with two different substrate orientations, one more along Fe—O bond axis (σ-like channel) and another one more perpendicular to Fe—O bond axis (π-like channel). For all these models, we revealed similar activation barriers. Thus, we concluded that both substrate approaches to all three geometries are competent in hydrogen atom abstraction. This corroborates our previous conclusions that the *S*=2 state provides the flexibility in HAA reactivity to $Fe^{IV}O$ complexes.

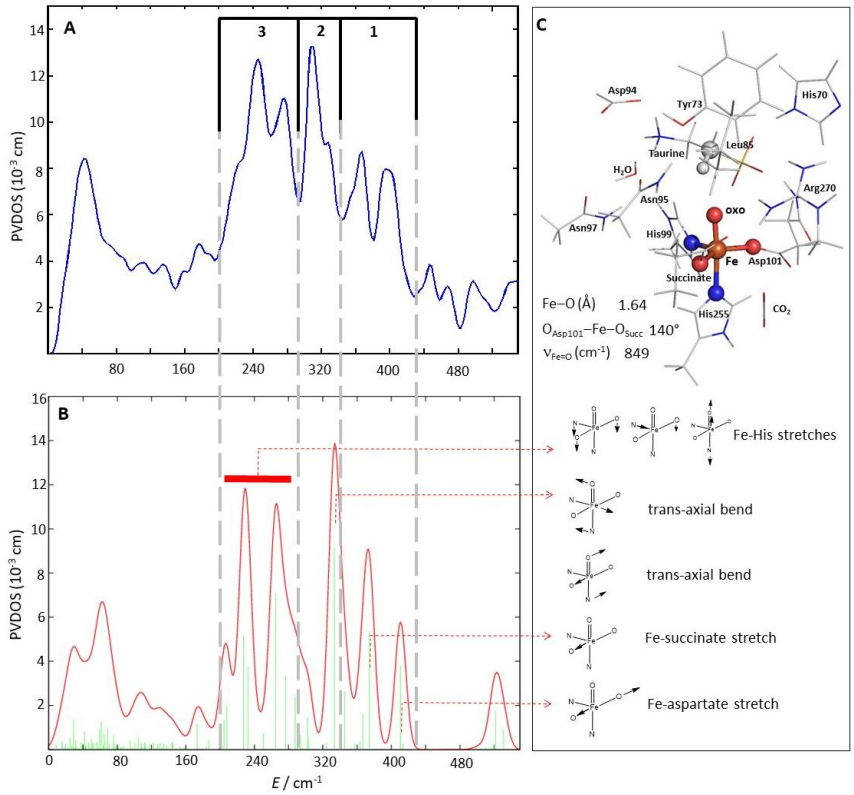

Figure 2.2-2: Experimental nuclear resonance vibrational spectrum (NRVS) of the Fe^{IV}=O intermediate of taurine dioxygenase (A) and the calculated NRVS (B) of the best (trigonal bipyramidal, TBP) structural candidate (C). Figure taken from Ref. 21.

2.3 The Fe^{IV}=O Active Site in Syringomycin Halogenase: Spectroscopy and Caclulations and the Definition of Geometric and Electronic Contribution to HAA-Controlled Chlorination Selectivity.

- *Wong S. D., **Srnec M.**, Matthews M. L., Liu L. V., Kwak Y., Park K., Bell C. B., Alp E. E., Zhao J., Yoda Y., Kitao S., Seto M., Krebs C., Bollinger Jr. J. M., Solomon E. I.: Elucidation of the Iron(IV)-Oxo Intermediate in the Non-Haem Iron Halogenase SyrB2. **Nature** 2013, 499, 320-323.*
- ***Srnec M.**, Wong S. D., Matthews M. L., Krebs C., Bollinger J. M., Solomon E. I.: Electronic Structure of the Ferryl Intermediate in the α-Ketoglutarate Dependent Non-Heme Iron Halogenase SyrB2: Contributions to H-atom Abstraction Reactivity. **J. Am. Chem. Soc.** 2016, 138, 5110-5122.*
- ***Srnec M.**, Solomon E. I.: Frontier Molecular Orbital Contributions to Chlorination versus Hydroxylation Selectivity in the Non-Heme Iron Halogenase SyrB2. **J. Am. Chem. Soc.** 2017, 139, 2396-2407.*

In analogy to NRVS/DFT determination of the structure of (TauD)Fe^{IV}O, we also determined the structure of the Fe^{IV}O intermediate in halogenase SyrB2. We found the Fe center to be in a trigonal bipyramidal configuration, with an axial Fe^{IV}=O bond (**Fig. 2.3-1**). The local structure of the ferryl in SyrB2 is therefore similar to (TauD)Fe^{IV}O. Moreover, we found that the DFT-calculated reaction coordinate for the O_2 activation pathway in the presence of the native substrate (following **Scheme 1**) reproduces this ferryl structure and places the substrate C-H bond perpendicular to the Fe—O vector. This result implies H-atom abstraction from the native substrate proceeds via the π channel (**Fig. 2.3-1**).

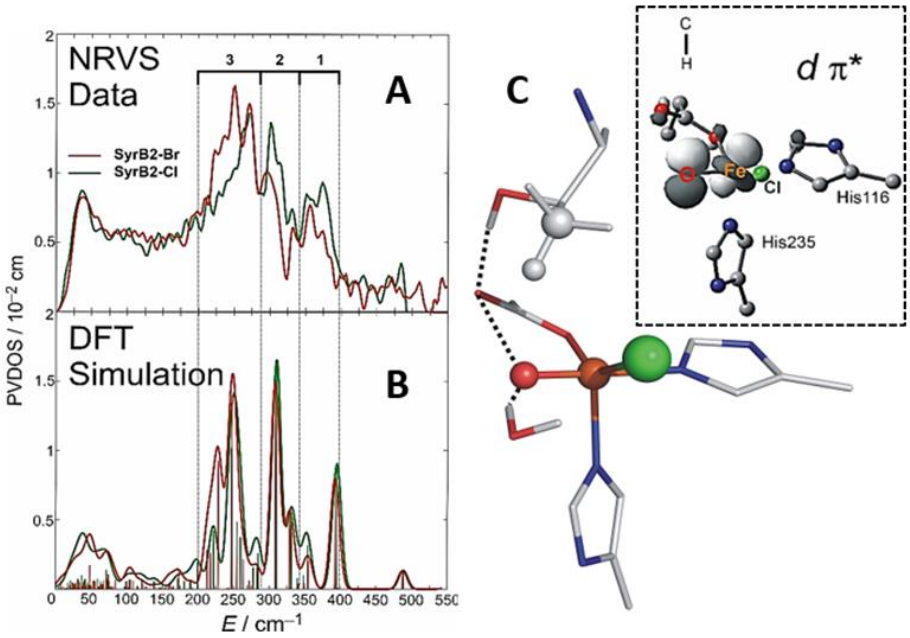

Figure 2.3-1: Experimental nuclear resonance vibrational spectrum (NRVS) of the Fe^{IV}=O intermediate of SyrB2 (A) and the caclulated NRVS (B) of the best structural candidate (C). One of the frontier molecular orbitals dπ* resposible for HAA is also shown. Figure adopted from Ref. 5.

Knowing the geometric structure of (SyrB2)$Fe^{IV}O$, we then used LT MCD spectroscopy in combination with quantum-chemical calculations to define the electronic structure. First, it appeared that LT MCD spectrum of (SyrB2)$Fe^{IV}O$ exhibits features similar to MCD of the (TMG_3tren)$Fe^{IV}O$ model from **section 2.1**. However, quantitative differences between MCDs of synthetic model and enzymatic active site (*cf.* **Fig. 2.1-1** vs. **Fig. 2.3-2**) are observed, evincing π-anisotropy and oxo donor strength that perturb frontier molecular orbitals in enzyme. Due to π-anisotropy (**Fig. 2.3-2**, *right*), the enzymatic Fe^{IV}═O active site exhibits enhanced reactivity in the direction of the substrate cavity that proceeds through a π-channel that is controlled by perpendicular orientation of the substrate C–H bond relative to the halide–Fe^{IV}═O plane.

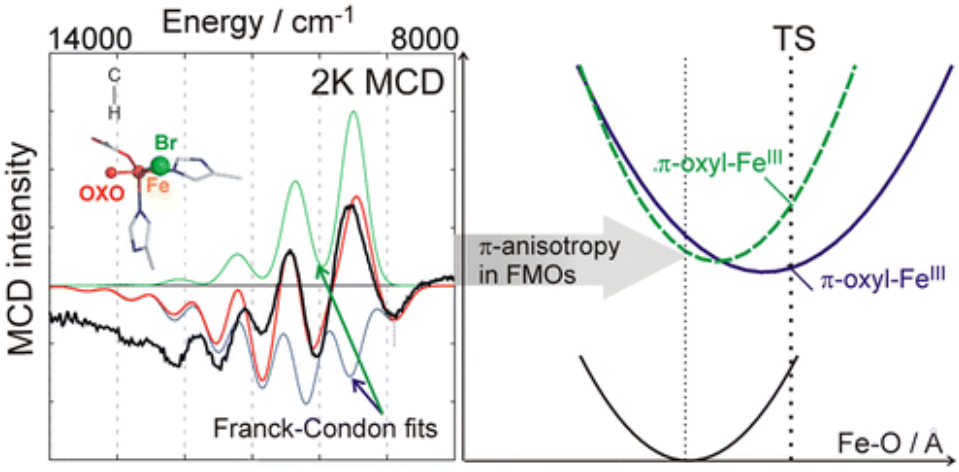

Figure 2.3-2: Vibronic structure of near infrared magnetic circular dichroism (NIR MCD) spectrum of the Fe^{IV}=O intermediate of syringomycin halogenase (*left*) and the caclulated potential energy surfaces PESs (*right*) associated with the NIR MCD feature. Two excited PESs are different despite the fact that both correspond to the dπ*→dσ* excitation. This indicates an anisotropy in these dπ* frontier molecular orbitals (FMOs). Figure taken from Ref. 22.

Having elucidated geometric and electronic properties of the (SyrB2)Fe^{IV}=O, we investigated the factors controlling reaction selectivity that is chlorination vesrus hydroxylation (second half of the catalytic cycle in **Scheme 1**). The π-channel for HAA was found to lead to the *S*=2 HO−Fe^{III}−Cl complex with the carbon-centered substrate radical, π-oriented relative to both Cl^- and OH^- ligands. In this configuration, chlorination becomes effectively competitive with hydroxylation that is otherwise thermodynamically more favored. Chlorination vs. hydroxylation selectivity is then determined by the orientation of the substrate with respect to the HO−Fe−Cl plane that controls either chloride or hydroxide to rebound depending on the relative π-overlap with the carbon-centered substrate radical (**Fig. 2.3-3**).

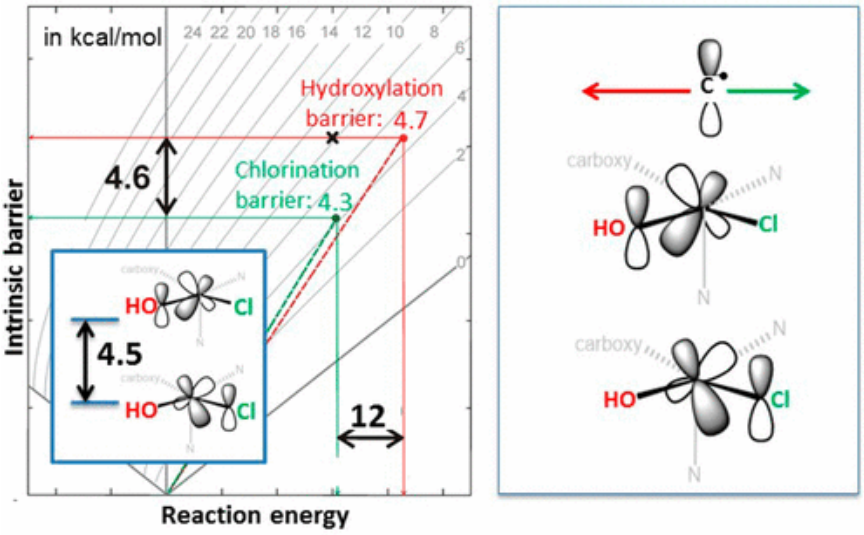

Figure 2.3-3: Despite a more favorable reaction energy for OH rebound (hydroxylation), the barrier for Cl rebound (halogenation) is somewhat lower due to a considerably smaller (Marcus-type) intrinsic barrrier (*left*) that is associated with the lower frontier molecular orbital, active in the Cl rebound process (*right*). Figure taken from 23.

3. Polynuclear Transition Metal Chemistry

One of enigmatic non-heme diiron enzymes, Δ^9 desaturase, the catalytic cycle of which I have intensively studied for more than one decade in collaboration with the groups of Prof. L. Rulíšek and Prof. E. I. Solomon, is presented in **section 3.1**. This binuclear non-heme iron system captivated our attention for its astonishing chemo-, regio- and stereo-selectivity, performing two subsequent H-atom abstrations from the „featureless“ stearoyl chain and inserting *cis* double bond between carbons 9 and 10. Over these years, our effort to elucidate chemistry of binuclear [FeFe] species produced “side” projects focused mostly on analysis of their electronic structure properties. This led us to the formulation of novel and insightful entanglement analysis of exchange coupling between magnetic centers in polynuclear transition metal complexes, as presented in **section 3.2**.

3.1 Reaction Mechanism of Δ^9 Desaturase

- ***Srnec M.**, Rokob T. A., Schwarz J., Kwak Y., Rulíšek L., Solomon, E. I.: Structural and Spectroscopic Properties of the Peroxodiferric Intermediate of Ricinus Communis Soluble Δ^9 Desaturase. **Inorg. Chem.** 2012, 51, 2806-2820.*
- *Chalupský J, Rokob A. T., Kurashige Y., Yanai T., Solomon E. I., Rulíšek L., **Srnec, M.**: Reactivity of the Binuclear Non-Heme Iron Active Site of Δ^9 Desaturase Studied by Large-Scale Multireference Ab Initio Calculations. **J. Am. Chem. Soc.** 2014, 136, 15977-15991.*
- *Bím D., Chalupský J., Culka M., Solomon E. I., Rulíšek L., **Srnec M.**: Proton-Electron Transfer to the Active Site Is Essential for the Reaction Mechanism of Soluble Δ^9 Desaturase**. J. Am. Chem. Soc.** 2020, 142, 10412-10423.*

Δ^9D is an O_2-dependent binuclear non-heme iron enzyme that evolved to convert stearic acid to oleic acid as a part of the fatty-acid metabolic pathway of plants.[24] In collaboration with the

spectroscopic group of Prof. E. I. Solomon, we initially focused on early stages of O_2 activation.[25a] Namely, we characterized geometric and electronic structure of the peroxy differic intermediate denoted as "**P**" (depicted on top of **Fig. 3.1-1**) combining density functional theory (DFT) calculations with data obtained from circular dichroism, resonance Raman and Mössbauer spectroscopies. Two follow-ups, which we published in the course of 6 years in JACS[25b,c], were mostly dealing with the exploration of several reaction pathways in order to complete the catalytic cycle. We employed hybrid DFT/molecular mechanics (DFT/MM) calculations, which we complemented for key reaction steps by advanced multiconfigurational and multireference calculations.

With that, we revealed several possible activations of **P**, including proton-assisted, O−O cleavage, and electron−proton transfer (EPT)-assisted pathways. From our calculations, we eventually favored the EPT-assisted activation of the **P**, which results into HAA-reactive intermediate (right part of **Fig. 3.1-1**) capable of abstracting H-atom from the substrate with barrier of only ~10 kcal mol^{-1} and with transition state to be only ~13 kcal mol^{-1} above the referential **P** intermediate. Additionally, computed data and postulated proton-transfer (PT) and electron-transfer (ET) pathways for the EPT-assisted mechanism of **P** activation were also corroborated by extensive bioinformatics study of various binuclear non-heme iron enzymes as well as different plant, archaeal, and bacterial desaturases.[25] It is a noticeable that the mechanism proposed by me and coworkers was experimentally corroborated through rational mutagenesis.[26]

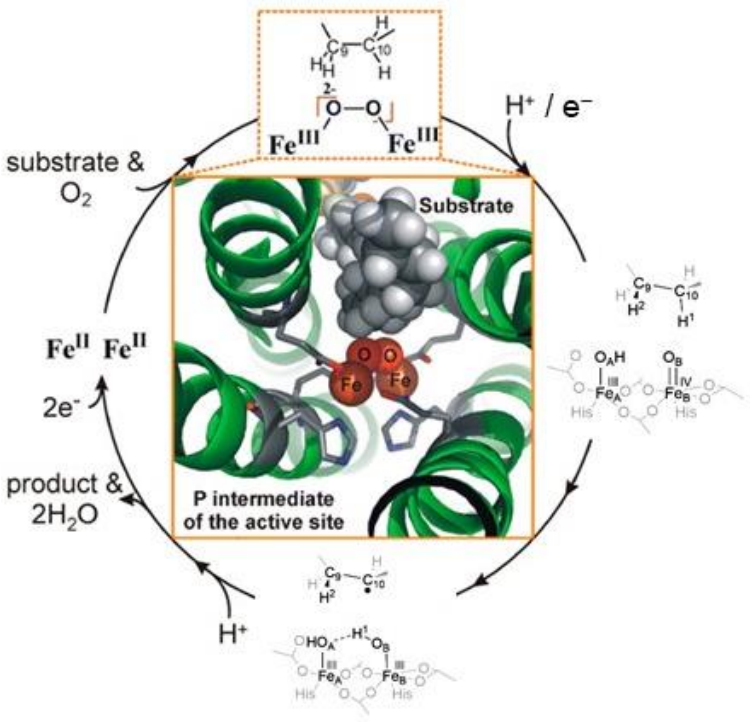

Figure 3.1-1: Catalytic cycle for binuclear non-heme iron desaturase Δ^9D proposed based on our computational studies.[25]

3.2 Novel Analysis of Magnetic Interactions in Polynuclear Transition Metal Complexes

- *Chalupský J,* ***Srnec M.****, Yanai T.: Interpretation of Exchange Interaction through Orbital Entanglement****. J. Phys. Chem. Lett.*** *2021, 12, 1268–1274.*
- *Chalupský J.,* ***Srnec M.****: Beyond the Classical Contributions to Exchange Coupling in Binuclear Transition Metal Complexes.* ***J. Phys. Chem. A*** *2021, 125, 2276–2283.*

Complexes with two (or more) spin-coupled open-shell metal ions usually have a very complex electronic structure with a number of exchange pathways coupling the magnetic sites. This also holds true for models of biologically important [FeFe] active sites such as the **P** intermediate of Δ^9D, the **X** intermediate of ribonucleotide reductase (bis-μ-oxo $Fe^{III}Fe^{IV}$), the **Q** intermediate of methane monooxygenase (bis-μ-oxo $Fe^{IV}Fe^{IV}$) etc. On the example of the **X** and **Q** models and five other bis-μ-oxo complexes, we specifically showed that an orbital-entanglement analysis of the configuartion interaction and density matrix renormalization group (DMRG) wavefunctions that is based on two-electron density (denoted by us as the T entanglement) serves as a simple and very insightful tool for identification of pathways contributing to the exchange (*J*) coupling between magnetic centers.[27]

It is also noteworthy that analysis of single-orbital entropy and mutual information has been recently introduced as a tool for the investigation of contributions to the exchange coupling between open-shell metal ions.[28] However, as we demonstrated in Ref. 27a, such an orbital-entanglement analysis may lead to an incorrect interpretation of the *J*-coupling mechanism, as opposed to our two-electron density based formulation of the orbital entanglement.

4. Computational Electrochemistry and Application to H-atom Abstraction Reactivity

My initial focus on reaction mechanisms of metalloenzymes and biomimetics, part of which I presented in **sections 2** and **3**, drifted me to the field of computational electrochemistry due to fact that all the catalysts studied in my laboratory, are redox active, and electron transfers (ETs) or concerted electron-proton transfers (CEPTs) are usually key steps along their catalytic pathway.

Throughout the past decade, theoretical chemistry has become an integral part of many electrochemical studies[29,30] and, hand in hand with it, enormous effort has been directed toward developing computational protocols for calculations of reduction potentials[29] that are defined as a Gibbs free-energy difference between the oxidized and reduced states (G_{ox} and G_{red}) in a given solvent, with respect to the absolute potential of a reference electrode:

$$E°[\mathrm{V}] = G_{ox}[\mathrm{eV}] - G_{red}[\mathrm{eV}] - E°_{abs}\,(\mathrm{reference})[\mathrm{eV}] \quad (1)$$

Different Gibbs free-energy evaluation strategies have been developed for various levels of structural complexity.[31,32,33] In **section 4.1**, I describe our contribution that is largely based on the calculation of free energies associated with addition(s) or abstraction(s) of hydrogen atom(s) to or from a chemical species, which eventually allows to evaluate its one-electron reduction potential, differently from eq 1. This study drifted further my focus on various physico-chemical aspects of CEPT reactions, which resulted in the formulation of an original and unique theoretical framework aiming at the prediction of CEPT reactivity from thermodynamics. In its current form, the framework features two thermodynamic factors that we named asynchronicity and frustration that together modulate concerted proton-electron transfer reactivity. Only after addition of these two factors to the classical well-documented effect known as linear free energy relationship (LFER capturing the effect of reaction energy on the barrier), a complete thermodynamic basis for the control of reactivity/selectivity is formed. Asynchronicity lowers the reaction barrier (increasing the reaction rate) so that a more asynchronous reaction gets faster, whereas frustration acts on the barrier in the opposite way so that a more frustrated reaction gets slower.

4.1 Methodological Development for Calculation of Reduction Potentials

- *Bím D., Rulíšek L.,* ***Srnec M.****: Accurate Prediction of One-Electron Reduction Potentials in Aqueous Solution by Variable Temperature H-atom Addition/Abstraction Methodology.* ***J. Phys. Chem. Lett.*** *2016, 7, 7-13.*

We devised an implicit solvation-based approach for calculating the reduction potential of a charged complex. The basic motivation for this development was to maintain the simplicity of the implicit solvation model and at the same time to avoid the largest source of errors in the prediction of the reduction potential resulting from the inaccurate description of the solvation energy in the continuum model (especially, solvation in aqueous medium is considered to be very difficult to capture).

The essential of the approach is illustrated by **Fig. 4.1-1**: to obtain the reduction potential of the charged MnO_4^- species ($E_2°$), the reduction potential of its neutralized (protonated) form MnO_3OH^0 ($E_1°$) is calculated first. Solvation energy of such a neutralized form within the implicit solvation model is presumably described more accurately than that of MnO_4^-. In the second step, the free energy difference between MnO_4^- and its hydrogenated form, MnO_3OH^{1-} (ΔG_{diag} – **Fig. 4.1-1**, *left*) is calculated at different temperatures and plotted as $\Delta G_{diag}(T)/T$ against $1/T$ (**Fig. 4.1-1**, *right*). Again, the description of the solvation energy of equally charged species in the implicit solvation model is assumed to be comparably (in)accurate and hence ΔG_{diag} to be less affected by the error in solvation than directly calculated $E_1°$. From the $\Delta G_{diag}(T)/T$ vs. $1/T$ plot, the slope of the linear dependence (ε) is obtained. This eventually allows to express $E_2°$ as a function of $E_1°$ and ε. Here, note that the trick with the temperature dependence of H-atom abstraction or

addition, which allows to separate redox and acidobasic contributions to ΔG_{diag}, is based on assumption that the acidobasic contribution is the only term that depends explicitly on temperature due to the *RT* factor. The accuracy of the method has been assessed for a set of 15 transition-metal complexes in aqueous medium, for which the results were found to be in very good agreement with experimental electrochemical data.

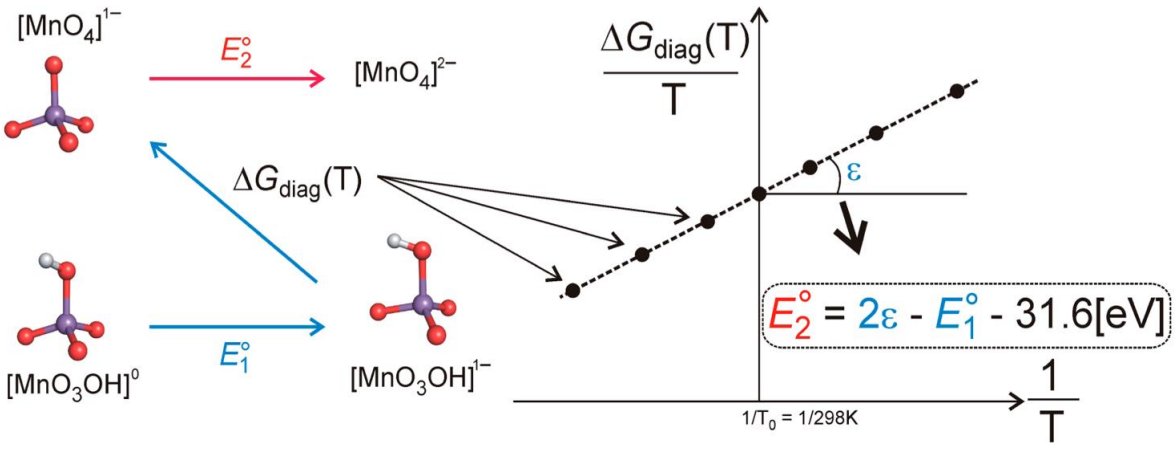

Figure 4.1-1: Computational protocol for prediction of the reduction potential of a negatively (or positively) charged complex ($E_2°$) by means of the reduction potential of its protonated (or deprotonated) counterpart ($E_1°$). As an example, the reduction potential calculation for MnO_4^- is schematically depicted. Figure taken from 34.

4.2 Asynchronicity Factor and Its Effect on CEPT Reactivity

- *Bím D., Maldonado-Domínguez M., Rulíšek L.,* ***Srnec M.*** *Beoynd the classical thermodynamic contributions to hydrogen atom abstraction reactivity.* ***Proc. Natl. Acad. Sci. U.S.A.*** *2018, 115, E10287-E10294.*
- *Bím D., Maldonado-Domínguez M., Fučík R.,* ***Srnec M.****: Dissecting the Temperature Dependence of Electron-Proton Transfer Reactivity.* ***J. Phys. Chem. C*** *2019, 123, 21422-21428.*

The concept of asynchronicity loosely arose from my methodological studies on reduction potentials from **section 4.1** because it is based on the interplay between redox and acidobasic components of the thermodynamic driving force of the CEPT reaction.

The concept is based on the quantities associated with the half-reaction thermodynamic cycle of a CEPT reactant (**Fig. 4.2-1**) that introduces two one-electron reduction potentials ($E°$ and $E°'$), two acidity constants ($pK_{a,Ox}$ and $pK_{a,Red}$) and proton-coupled reduction potential ($E°_H$). These key quantities are further utilized to define effective reduction potential ($E°_{eff}$) and effective acidity constant ($pK_{a,eff}$) as also shown in **Fig. 4.2-1**.

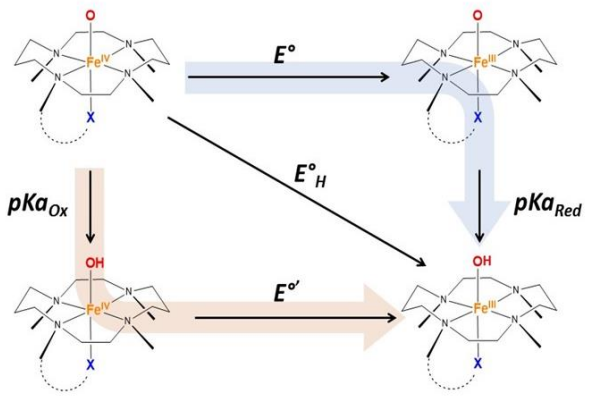

$$E^\circ_{\text{eff}} = \tfrac{1}{2}(E^\circ + E^{\circ\prime})$$

$$pK_{\text{a,eff}} = \tfrac{1}{2}(pK_{\text{a,red}} + pK_{\text{a,ox}})$$

Figure 4.2-1: Thermodynamic cycle of the CEPT half reaction along with the four thermodynamic quantities – two reduction potentials (E° and $E^{\circ\prime}$) and two acidity constants ($pK_{\text{a,ox}}$ and $pK_{\text{a,Red}}$) (*left*). Definition of the effective reduction potential and acidity constant based on the cycle (*right*), which is further used in the concept of asynchronicity.

Employing the *effective* quantities, E°_{H} and the parameter ω can be defined on the same footage (right panel in **Fig. 4.2-2**). While E°_{H} is the measure of the ability of a system to acquire a hydrogen atom, ω represents a descriptor capturing a relative magnitude of the redox vs. acidobasic component of E°_{H}. Transformation of the [E°_{eff}, $RT/F\ln(10)\times pK_{\text{a,eff}}$] pair into the E°_{H} and ω quantities is visualized in **Fig. 4.2-2** (*left*). In the plot, a [$E^\circ_{\text{H}}/\omega$] data point falling below the main diagonal (the E°_{H} axis) has a dominant redox component of E°_{H}, whereas the area above the diagonal is characterized by a dominancy of the acidobasic component.

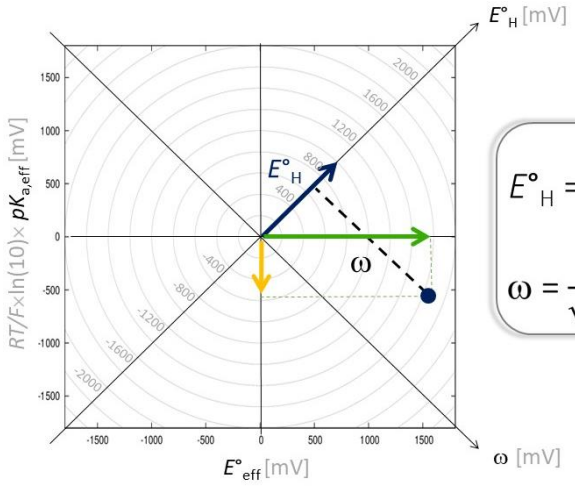

$$E^\circ_{\text{H}} = E^\circ_{\text{eff}} + RT/F\times\ln(10)\times pK_{\text{a,eff}}$$

$$\omega = \frac{1}{\sqrt{2}} \times (E^\circ_{\text{eff}} - RT/F\times\ln(10)\times pK_{\text{a,eff}})$$

Figure 4.2-2: Propensity of the system to acquire a hydrogen atom is quantified by proton coupled reduction potential (E°_{H}), while the disparity between acidobasic and redox components of E°_{H} is described by the parameter ω.

An analogous plot to **Fig. 4.2-2** dealing with differences in E°_{H} and ω between the two reactants ($\Delta E^\circ_{\text{H}}$ and in $\Delta\omega$) is shown in **Fig. 4.2-3**. While $\Delta E^\circ_{\text{H}}$ accounts for the free energy of

reaction, which is the thermodynamic driving force for any CEPT reaction, the quantity $\Delta\omega$ is a measure of the disparity between thermodynamic driving forces for electron vs. proton transfer that contribute (un)equally to $\Delta E°_H$. Hence, the parameter $\Delta\omega$ (further denoted as η) is the factor of asynchronicity. In **Fig. 4.2-3**, any $[\Delta E°_H/\eta]$ point appearing in the right quarter-square triangle is associated with an exergonic CEPT reaction with asynchronicity in favor of ET, while an exergonic reaction in a favor of PT is featured by a point lying in the top quarter-square triangle. The triangle below the η axis is the zone for endergonic CEPT reactions.

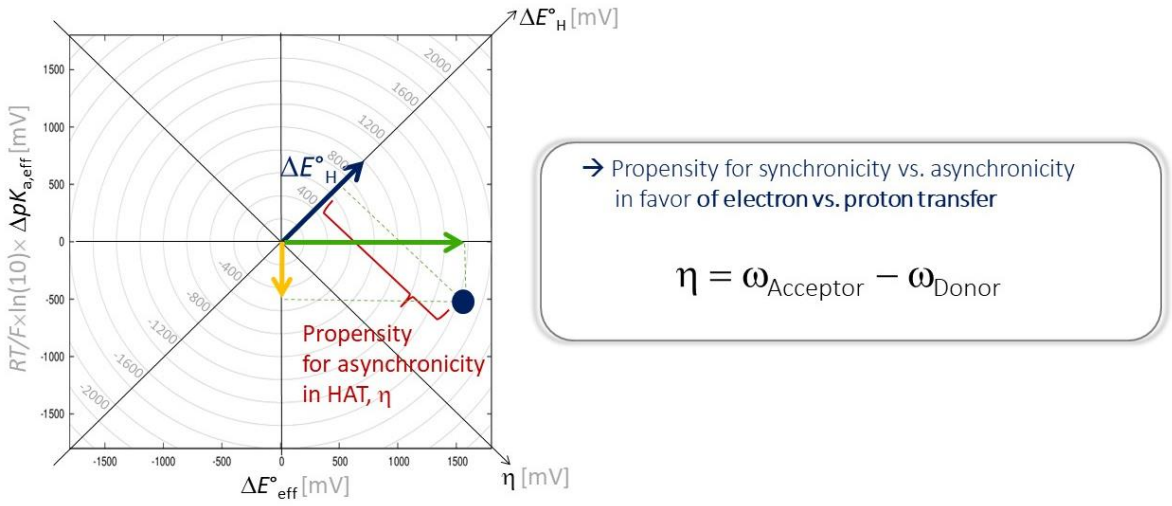

Figure 4.2-3: The CEPT thermodynamic driving force is quantified as a difference between proton coupled reduction potentials of an oxidant (H-atom acceptor) and a substrate (H-atom donor) - $\Delta E°_H$, while the parameter η measures the disparity between acidobasic and redox component of such a thermodynamic driving force and is given as a difference between the parameters ω for both H-atom acceptor and donor.

To link asynchronicity with chemical reactivity, we employed Marcus-type model for reaction barrier. In the framework of this model, we eliminated the effect of reaction free energy on the barrier (that is LFER: $\Delta G_0/2 \equiv -F\times\Delta E°_H/2$; F – Faraday constant). This allowed us to focus on the effect of η on reorganization energy λ - one of two key quantities (along with ΔG_0) co-determining the free-energy barrier. Specifically, we found that η can be expressed as a part of λ so that λ equals to $\lambda_0 - F|\eta|$, where λ_0 is interpreted as reorganization energy at the synchronous limit. Note that 'similar' CEPT reactions share the same synchronous limit λ_0. According to the relationship between λ and η, reorganization energy reaches its maximum at the synchronous limit. Thus, increasing asynchronicity in any of two possible directions ($\eta < 0$ or > 0) lowers the free-energy barrier by $-F|\eta|/4$ (provided all other variables such as λ_0 and ΔG_0 remain unchanged; a prefactor of ¼ comes from Marcus theory).

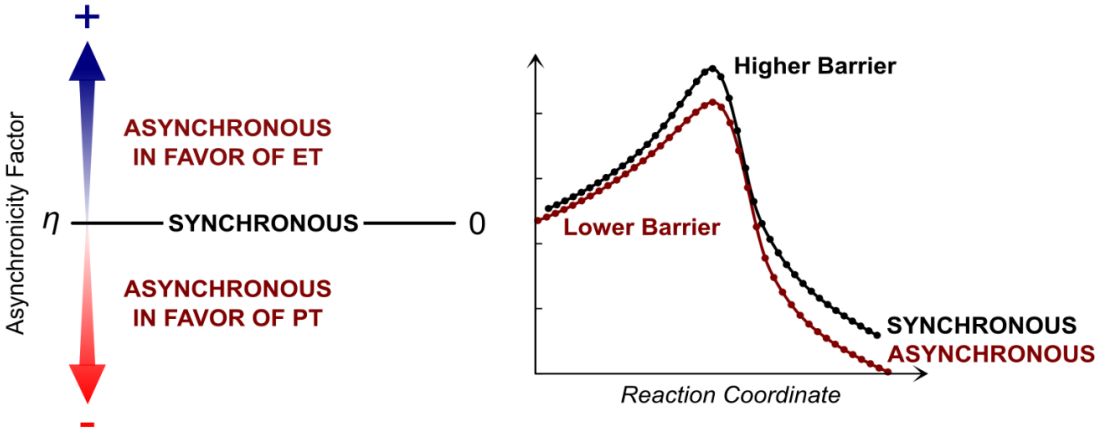

Figure 4.2-4: Variation of the parameter η controls asynchronicity between ET and PT in the concerted electron-proton transfers, which also affects the reaction barrier so that a CEPT reaction with a higher asynchronicity in favor of ET or PT tends to have a lower barrier. Figure adopted from Ref. 35.

Using the cocept of asynchronicity, we studied a rare case of an inverse *T*-dependence of a single-step reaction, which slows down as temperature increases. We demonstrated asynchronicity as one of a few factors that tips the balance in favor of the inverse *T*-dependence of the CEPT reaction between the $Fe^{II}(H_2bip)_3$ complex ($H_2bip \equiv$ 2,2-bi-1,4,5,6-tetrahydropyrimidine) and the TEMPO radical (2,2,6,6-tetramethyl-1-piperidinoxyl) reported by Mayer *et al*.[36]

To conclude the section on asynchronicity, the presented concept of asynchronicity has been used by several experimental groups to rationalize/explain otherwise non-intuitive observations (Ref. 37, 38). Encouraged by this fact, I forsee asynchronicity to be an indispensable tool for a control of CEPT reactivity, which may simplify chemical procedures for selective C-H bond functionalization that usually require many steps (such as the installation and removal of protecting or directing groups).

4.3. Concept of Asynchronicity Extended by Including Frustration Factor.

- *Maldonado-Domínguez M.,* ***Srnec M.****: H-atom Abstraction Reactivity through the Lens of Asynchronicity and Frustration with their Counter-Acting Effects on Barriers.* ***Inorg. Chem.*** *2022, 61, 18811–18822. ACS Editor's Choice).*
- *Maldonado-Domínguez M.,* ***Srnec M.****: Quantifiable polarity match effect on C-H bond cleavage reactivity and its limits in reaction design.* ***Dalton Trans.*** *2023, 52, 1399-1412.*

The transformation of the basis formed by the reduction potential and the acidity constant ($E°_A$ and $pK_{a,A}$) of the oxidant A• yields the couple of thermodynamic functions ω and μ as shown in **Fig. 4.4-1**. The meaning of ω, denoted as *potential disparity* of A•, was already explained in **section 4.2**. As such, it measures the potential of A• to be stronger/weaker oxidant than base. The parameter μ, denoted as *potential duality* of A•, measures the potential of A• to act as a strong/weak oxidant and

base together (*ie.*, strong/weak oxidizing base). Then, the difference between the parameters ω of two species X• and Y• competing over an H-atom is a measure of asynchronicity (**Fig. 4.4-1**, *left lower panel*), while the difference between the parameters μ determines the so-called frustration of CEPT reaction ($\sigma \equiv \Delta\mu$). Any CEPT reaction is thus characterized by three thermodynamic variables – reaction energy ($\Delta E°_H$), asynchronicity (η) and frustration (σ) as shown in **Fig. 4.4-1** (*right*).

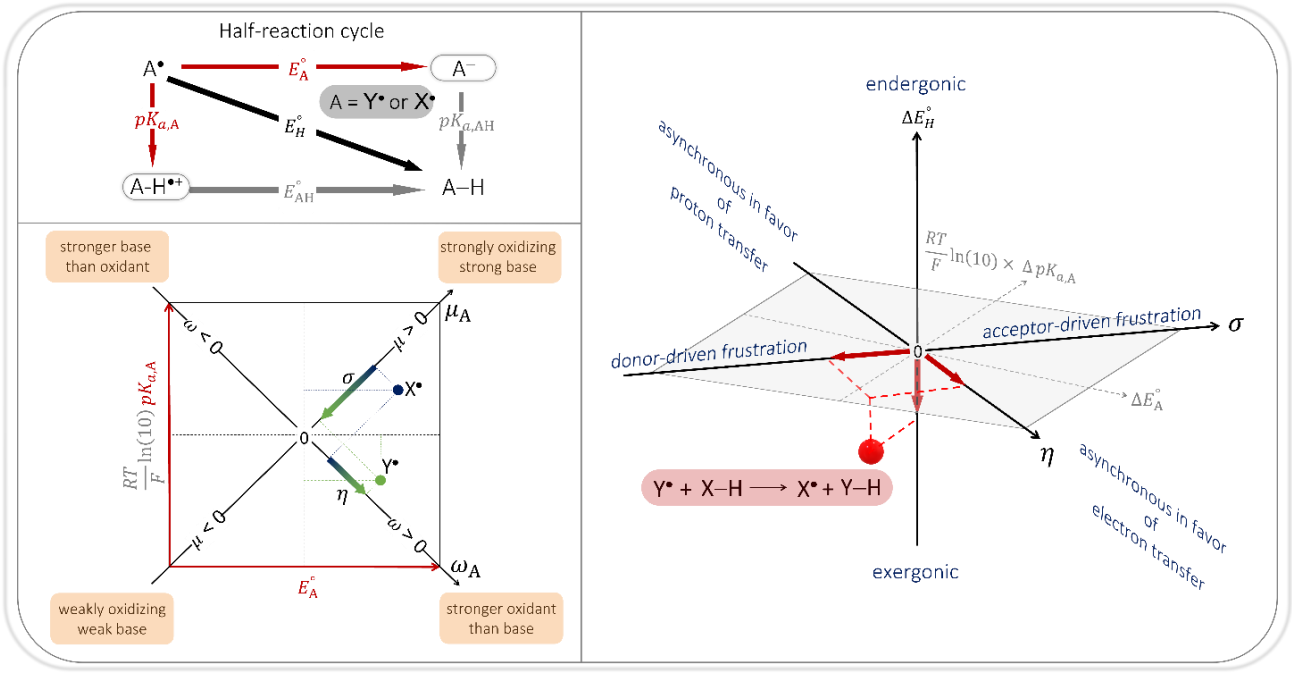

Figure 4.4-1. *Left Upper Panel*: Thermodynamic characterization of the H-atom acceptor A• and its hydrogenated form AH. *Left Lower Panel:* Transformation of the [$E°_A$/$pK_{a,A}$] coordinate system (axes in red) into the system with the [ω/μ] coordinates. *Right Panel:* A complete thermodynamic basis for the description of reaction Y• + X–H → Y–H + X• is composed of three variables: η, σ, and $\Delta E°_H$. Figure taken from Ref. 39.

In analogy to asynchronicity, we discovered the effect of frustration on the CEPT barrier. As a result, the expression for the linearized Marcus-type model of the barrier, which explicitly accounts for all three thermodynamic components (LFER, η and σ), reads:

$$\Delta G^{\neq}_{\text{Marcus}} = \frac{\lambda_{00}}{4} + \frac{\Delta G_0}{2} + \frac{F}{4}(|\sigma| - |\eta|) \qquad (2)$$

where $\lambda_{00}/4$ stands for double-zero (synchronous and unfrustrated) limit for intrinsic barrier. Only after addition of the three factors LFER, $|\eta|/4$ and $|\sigma|/4$, a complete thermodynamic projection on reactivity is formed. In principle, the appropriate combination of $|\eta|/4$ and $|\sigma|/4$ factors is potent to change the preference for which X-H bond is likely to be activated, which would otherwise be governed by LFER favoring the weakest X-H bonds in molecules.

The robustness of the eq. (2) was tested on the six sets of HAA reactions reported in the literature as shown in **Fig. 4.4-2**, where the Pearson correlation coefficient r^2 improves as the three thermodynamic factors are gradually included.

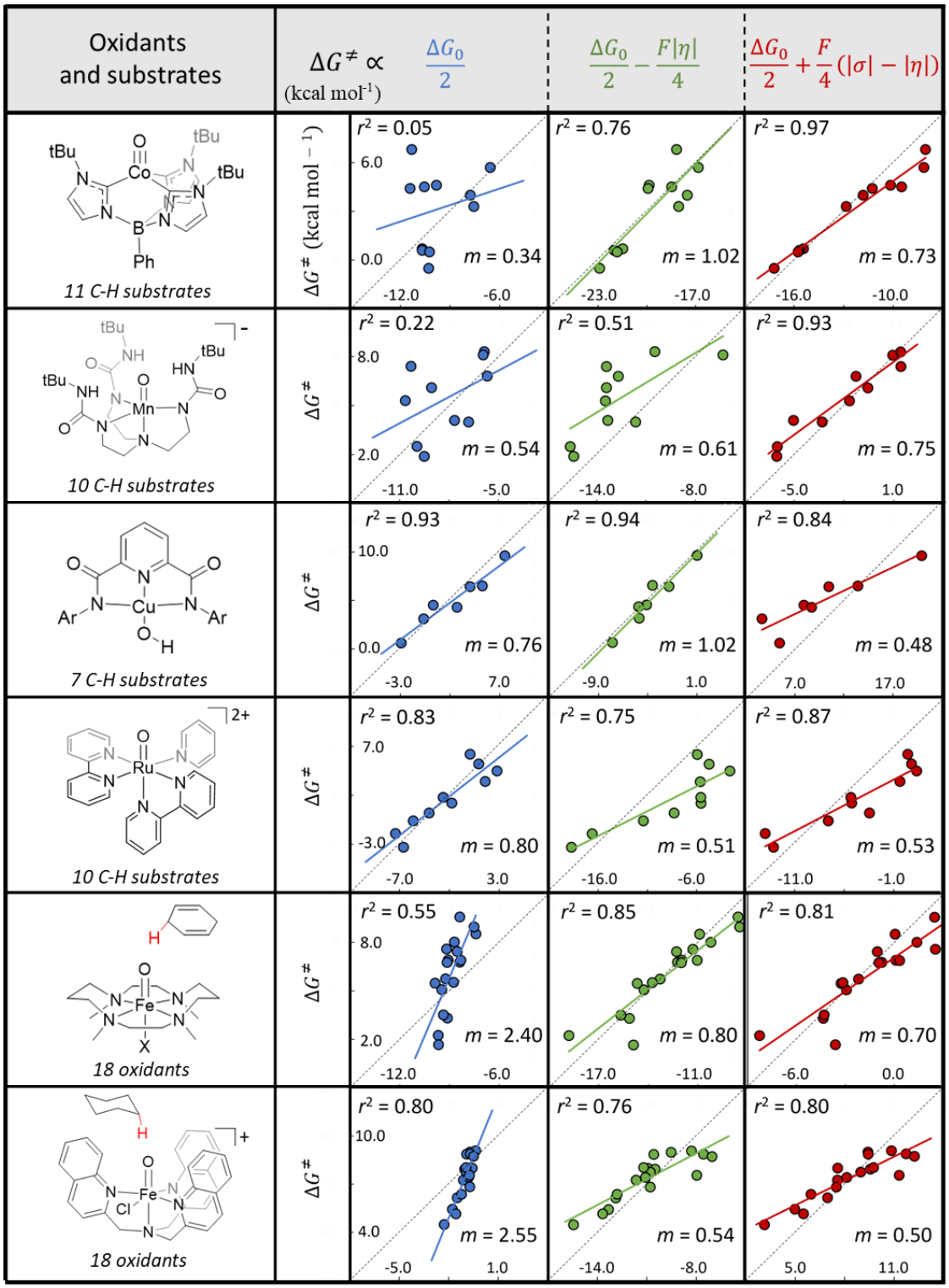

Figure 4.4-2. $\Delta G^{\neq}$ vs. LFER (blue); $\Delta G^{\neq}$ vs. LFER and asynchronicity effect (green); $\Delta G^{\neq}$ vs. LFER, asynchronicity and frustration effect (red) plotted for six reaction sets. Figure adopted from Ref. 39.

4.4 Kinetic Energy Distribution and its Relation to H-atom Abstraction Reactivity

- *Maldonado-Domínguez M., Bím, D., Fučík R., Čurík R., **Srnec M.**: Reactive mode composition factor analysis of transition states: the case of coupled electron-proton transfers. **Phys. Chem. Chem. Phys.** 2019, 21, 24912-24918. (2019 PCCP HOT Articles)*
- *Maldonado-Domínguez M., **Srnec M.**: Understanding and Predicting Post H-Atom Abstraction Selectivity through Reactive Mode Composition Factor Analysis. **J. Am. Chem. Soc.** 2020, 142, 3947-3958.*
- *Bharadwaz P., Maldonado-Domínguez M., **Srnec M.**: Bifurcating Reactions: Distribution of Products from Energy Distribution within a Shared Reactive Mode. **Chem. Sci.** 2021, 12, 12682-12694.*
- *Bharadwaz P., Maldonado-Domínguez M., Chalupský J., **Srnec M.**: Reactivity Factors in Catalytic Methanogenesis and their Tuning upon Coenzyme F430 Biosynthesis. **J. Am. Chem. Soc.** 2023, 145, 9039–9051.*

I and my team developed a simple method for the evaluation of the kinetic energy distribution (KED) within the reactive mode of a transition state and demonstrated its applicability by linking the KED with the asynchronicity in C–H bond activation as reported in Ref. 40. Also, we utilized a KED analysis for understanding post CEPT selectivity using a set of eight experimentally well-characterized synthetic $Fe^{IV}O$ complexes.[41] A control over selectivity of this type of biomimetics is challenging due to their high CEPT reactivity and their rich post-CEPT itinerary: H-atom abstraction from a substrate yields an Fe—OH moiety and a carbon-centered substrate radical that can further undergo various reaction transformations such as the radical hydroxylation by Fe—OH or the radical dissociation from Fe—OH. By quantifying KED within the reactive mode at TS_{CEPT}, the method allowed for the rationalization of the experimentally observed OH rebound vs. dissociation selectivity (**Fig. 4.4-1**). In addition, we also showed that both ΔG_0 and η of the CEPT step are the key thermodynamic parameters, which control the final product outcome upon ferryl-promoted C−H activation. Thus, the method allows qualitative predictions at low computational costs, providing guidelines to harness post-CEPT selectivity and demonstrating that experimental kinetic isotope effect can serve as a mechanistic probe in this context. It is noticeable that the conclusions from our unorthodox analyses were recently supported by a molecular dynamics study.[42]

For the sake of completeness, I also wish to mention two works employing KED for elucidation of some important reactivity features. First, we successfully applied the KED approach for evaluation of product branching ratios of nearly 50 organic 'bifurcating' reactions that always lead to two products after passing the only TS. This type of reactions cannot be obviously described by standard Eyring's transition state theory.[43] Second, we also employed KED analysis in the mechanistic study of the enzyme with the native F430 cofactor, responsible for CH_4 formation from two coenzymes B (CoBS-H) and M (H_3C-SCoM). Among other things, we found that the transition state displays the very high pro-reactive motion of the transient CH_3 fragment toward the H–S bond, superior to models with the F430 biosynthetic ancestors. This feature likely prevents from the formation of a deleterious radical intermediate.[44]

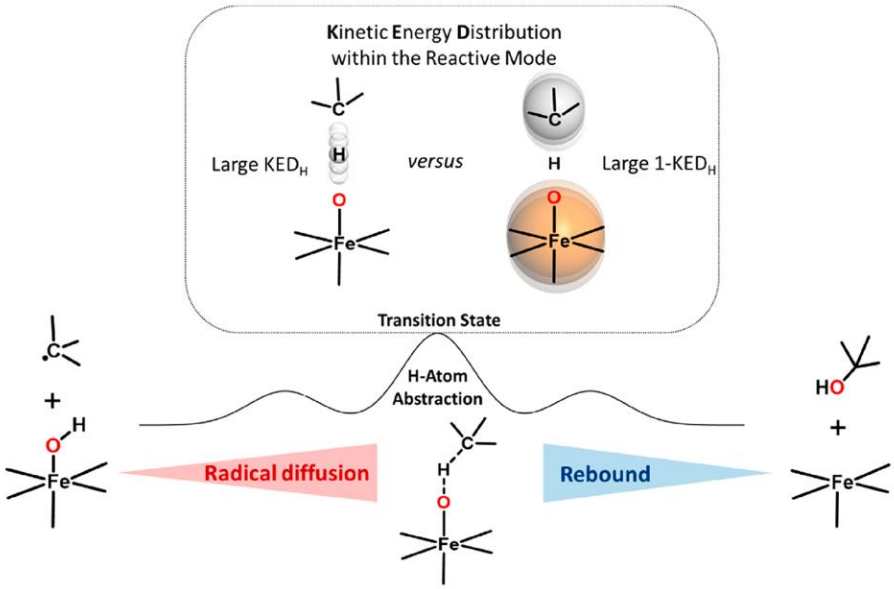

Figure 4.4-1: Post CEPT selectivity can be controlled by kinetic energy distribution (KED) in the reactive mode of CEPT transition state (TS_{CEPT}). The systems with a small fraction of kinetic energy on the transferred H atom (KED_H) at TS_{CEPT} undergo OH rebound, otherwise they dissociate. Figure take from Ref. 41.

5. Conclusion

All of the projects presented in the dissertation are related to the field of physical inorganic and bioinorganic chemistry and share one common theme: concerted electron-proton transfer (CEPT) reactions. These reactions correspond to key steps in catalytic cycles of many redox-active metalloenzymes. This includes mononuclear and binuclear non-heme iron enzymes, which have been subjected to my scientific interest for over 15 years. During this period, my research covered various aspects of their chemistry: (***i***) elucidation of active-site geometries of some key reactive intermediates using an arsenal of computational and experimental techniques; (***ii***) elucidation of the acive-site electronic structure properties through the correlation of quantum-chemical calculations with spectroscopic data; (***iii***) development of new analytical tools for the interpretation of complex wavefunctions; (***iv***) analysis of geometric and electronic contributions to reactivity and selectivity; (***v***) computational exploration of reaction mechanisms along the whole catalytic cycles; (***vi***) analysis of parallels and differences in reactivity between metalloenzymes and their biomimetics.

My activity in metalloenzymatic and related redox chemistry naturally brought my attention to computational electrochemistry, where I and my co-workers started with the attempts to develop a reliable and yet simple methodology for the calculation of a key electrochemical quantity – one-electron reduction potential. Encouraged by our initial success in this field, we turned our curiosity towards relationships between key components of the thermodynamic driving force in CEPT reactions – reduction potential and acidity constant. These studies led us to the formulation of the

concept of asynchronicty in CEPT reactions and the description of its effect on CEPT reactivity and selectivity. According to this concept, a more pronounced disparity between redox and acidobasic components of thermodynamic driving force leads to a larger reduction of CEPT reaction barrier (considering the non-tunneling regime) and hence an increased reaction rate. This effect is quantifiable through the implemention of the asynchronicity factor into the Marcus-type reaction barrier. Since our pioneering work, which was experimentally justified by the group of Prof. Anderson from University of Chicago,[37] we have already applied the concept to various chemical problems. Furthermore, we extended the concept by completing the thermodynamic effect on the CEPT barrier by introducing the factor of frustration and continue with the development of the concept in order to overcome its limitations associated with the applicability of Marcus-type theory in CEPT space so that this may become an integral part of chemistry.

The analysis of kinetic energy distribution (KED) within the reactive mode of a transition state is another aspect of CEPT chemistry that I pioneered. Importantly, we found that KED at transition state of a CEPT process may strongly affect the product outcome in cases, where CEPT opens more than one (post-CEPT) reactive channel with reasonably low barriers. In such cases, selectivity cannot be rationalized using the standard Eyring's transition state theory and is already encoded to a large extent in transition state of CEPT.

All of my contributions aim at understanding an interplay of various physico-chemical factors affecting CEPT and related processes, with the ambition to extend significantly our ability to make reactions more selective. This is a crucial prerequisite for more environmentally friendly, material and energy saving chemistry. Particularly, selective activation of aliphtic C–H bonds represents a real challenge for the current synthetic chemistry searching for routes with fewer and more productive steps. From this perspective, I forsee that our research on metalloenzymes and biomimetics with the CEPT process placed in the center of their catalytic function, as well as our concepts on CEPT reactivity provide insightful and quantitative guidelines for rational design of new effective catalysts.

References

(1) Rokob, T. A.; Chalupský, J.; Bím, D.; Andrikopoulos, P. C.; Srnec, M.; Rulíšek, L.: Mono and binuclear non-heme iron chemistry from a theoretical perspective. *J. Biol, Inorg. Chem.* **2016**, *21*, 619-644.

(2) a) Bruijnincx, P. C. A.; van Koten, G.; Klein Gebbink, R. J. M.: Mononuclear non-heme iron enzymes with the 2-His-1-carboxylate facial triad: recent developments in enzymology and modeling studies. *Chem. Soc. Rev.* **2008**, *37*, 2716-2744. b) Krebs, C.; Galonić Fujimori, D.; Walsh, C. T.; Bollinger Jr., J. M.: Non-Heme Fe(IV)-Oxo Intermediates. *Acc. Chem. Res.* **2007**, *40*, 484-492. c) Solomon, E. I.; Goudarzi, S.; Sutherlin, K. D.: O2 Activation by Non-Heme Iron Enzymes. *Biochemistry*, **2016**, *55*, 6363-6374.

(3) Solomon, E. I.; Light, K. M.; Liu, L. V.; Srnec, M.; Wong, S. D.: Geometric and Electronic Structure Contributions to Function in Non-heme Iron Enzymes. *Acc. Chem. Res.* **2013**, *46*, 2725-2739.

(4) Solomon, E. I. *et al.*: Geometric and Electronic Structure/Function Correlations in Non-Heme Iron Enzymes. Chem. Rev. 2000, 100, 235-350.

(5) Wong, S. D.; Srnec, M.; Matthews, M. L.; Liu, L. V.; Kwak, Y.; Park, K.; Bell, C. B.; Alp, E. E.; Zhao, J.; Yoda, Y.; Kitao, S.; Seto, M.; Krebs, C.; Bollinger Jr., J. M.; Solomon, E. I.: Elucidation of the Iron(IV)-Oxo Intermediate in the Non-Haem Iron Halogenase SyrB2. *Nature* **2013**, *499*, 320-323.

(6) Hammes-Schiffer, S.; Stuchebrukhov, A. A.: Theory of Coupled Electron and Proton Transfer Reactions. *Chem. Rev.* **2010***, 110*, 6939–6960.

(7) Tyburski, R.; Liu, T.; Glover, S. D; Hammarström, L.: Proton-Coupled Electron Transfer Guidelines, Fair and Square. *J. Am. Chem. Soc.* **2021**, *143*, 560–576.

(8) Hammes-Schiffer, S.: Theory of Proton-Coupled Electron Transfer in Energy Conversion Processes. *Acc. Chem. Res.* **2009***, 42*, 1881–1889.

(9) Costentin, C.; Savéant, J. M.: Hydrogen and proton exchange at carbon. Imbalanced transition state and mechanism crossover. *Chem. Sci.* **2020***, 11*, 1006-1010.

(10) Mandal, M. *et al.*: Mechanisms for Hydrogen-Atom Abstraction by Mononuclear Copper(III) Cores: Hydrogen-Atom Transfer or Concerted Proton-Coupled Electron Transfer? *J. Am. Chem. Soc.* **2019**, *141*, 17236-17244.

(11) Coste, S. C.; Brezny, A. C; Koronkiewicz, B.; Mayer, J. M.: C–H oxidation in fluorenyl benzoates does not proceed through a stepwise pathway: revisiting asynchronous proton-coupled electron transfer. *Chem. Sci*. **2021**, *12*, 13127-13136.

(12) Roberts, B. P.: Polarity-reversal catalysis of hydrogen-atom abstraction reactions: concepts and applications in organic chemistry. *Chem. Soc. Rev.* **1999**, *28*, 25-35.

(13) Kawamata, Y. *et al.*: Scalable, Electrochemical Oxidation of Unactivated C−H Bonds. *J. Am. Chem. Soc.* **2017**, *139*, 7448−7451.

(14) Sayfutyarova, E. R.; Goldsmith, Z. K.; Hammes-Schiffer, S.: Theoretical Study of C–H Bond Cleavage via Concerted Proton-Coupled Electron Transfer in Fluorenyl-Benzoates. *J. Am. Chem. Soc.* **2018***, 140*, 15641–15645.

(15) Parada, G. A. *et al.*: Concerted proton-electron transfer reactions in the Marcus inverted region. *Science* **2019**, *364*, 471-475.

(16) McDonald, A. R.; Que Jr., L.: High-valent nonheme iron-oxo complexes: Synthesis, structure, and spectroscopy. *Coord. Chem. Rev.* **2013**, *257*, 414-428.

(17) England, J.; Martinho, M.; Farguhar, E. R.; Frisch, J. R.; Bominaar, E. L.; Munck, E.; Que Jr., L.: A synthetic high-spin oxoiron(IV) complex: generation, spectroscopic characterization, and reactivity. Angew. Chem. Int. Ed. **2009**, *46*, 3622-3626.

(18) Srnec, M.; Wong, S. D.; England, J.; Que, Jr. L.; Solomon, E. I.: π-Frontier Molecular Orbitals in S=2 Ferryl Species and Elucidation of Their Contributions to Reactivity. *Proc. Natl. Acad. Sci. U.S.A.* **2012**, *109*, 14326-14331.

(19) Srnec, M.; Wong, S. D.; Solomon, E. I.: Excited state potential energy surfaces and their interactions in $Fe^{IV}O$ active sites. *Dalton Trans.* **2014**, *43*, 17567-17577.

(20) a) Price, J. C.; Barr, E. W.; Tirupati, B.; Bollinger, J. M.; Krebs, C.: The First Characterization of a High-Valent Iron Intermediate in the Reaction of an α-Ketoglutarate-Dependent Dioxygenase: A High-Spin Fe(IV) Complex in Taurine/α-Ketoglutarate Dioxygenase (TauD) from Escherichia coli. *Biochemistry* **2003**, *42*, 7497-7508. b) EXAFS spectroscopic evidence for an Fe=O unit in the Fe(IV) intermediate observed during oxygen activation by taurine: alpha-ketoglutarate dioxygenase. *J. Am. Chem. Soc.* **2004**, *126*, 8108-8109.

(21) Srnec, M.; Iyer, S. R.; Dassama, L. M. K.; Park, K.; Wong, S. D.; Sutherlin, K. D.; Yoda, Y.; Kobayashi, Y.; Kurokuzu, M.; Saito, M.; Seto, M.; Krebs, C.; Bollinger Jr, J. M.; Solomon, E. I.: Nuclear Resonance Vibrational Spectroscopy Definition of the Facial Triad FeIV=O Intermediate in Taurine Dioxygenase: Evaluation of Structural Contributions to Hydrogen Atom Abstraction. *J. Am. Chem. Soc.* **2020**, *142*, 18886-18896.

(22) Srnec, M.; Wong, S. D.; Matthews, M. L.; Krebs, C.; Bollinger, J. M.; Solomon, E. I.: Electronic Structure of the Ferryl Intermediate in the α-Ketoglutarate Dependent Non-Heme Iron Halogenase SyrB2: Contributions to H-atom Abstraction Reactivity. *J. Am. Chem. Soc.* **2016**, *138*, 5110-5122.

(23) Srnec, M.; Solomon, E. I.: Frontier Molecular Orbital Contributions to Chlorination versus Hydroxylation Selectivity in the Non-Heme Iron Halogenase SyrB2. *J. Am. Chem. Soc.* **2017**, *139*, 2396-2407.

(24) a) Nagai, J.; Bloch, K.: Enzymatic desaturation of stearyl acyl carrierprotein. *J. Biol. Chem.* **1968**, *243*, 4626−4633. b) Morris, L. J.: Mechanisms and stereochemistry in fatty acid metabolism. *Biochem. J.* **1970**, *118*, 681−693. c) Schmidt, H.; Heinz, E.: Involvement of Ferredoxin in Desaturation of Lipid-Bound Oleate in Chloroplasts. *Plant Physiol.* **1990**, *94*, 214−220. d) Wada, H.; Schmidt, H.; Heinz, E.; Murata, N.: In vitro ferredoxin-dependent desaturation of fatty acids in cyanobacterial thylakoid membranes. *J. Bacteriol.* **1993**, *175*, 544−547.

(25) a) Srnec, M.; Rokob, T. A.; Schwarz, J.; Kwak, Y.; Rulíšek, L.; Solomon, E. I.: Structural and Spectroscopic Properties of the Peroxodiferric Intermediate of Ricinus Communis Soluble Δ^9 Desaturase. *Inorg. Chem.* **2012**, *51*, 2806-2820. b) Chalupský, J; Rokob, A. T.; Kurashige, Y.; Yanai, T.; Solomon, E. I.; Rulíšek, L.; Srnec, M.: Reactivity of the Binuclear Non-Heme Iron Active Site of Δ^9 Desaturase Studied by Large-Scale Multireference Ab Initio Calculations. *J. Am. Chem. Soc.* **2014**, *136*, 15977-15991. c) Bím, D.;

Chalupský, J.; Culka, M.; Solomon, E. I.; Rulíšek, L.; Srnec, M.: Proton-Electron Transfer to the Active Site Is Essential for the Reaction Mechanism of Soluble Δ^9 Desaturase. *J. Am. Chem. Soc.* **2020**, *142*, 10412-10423.

(26) Tupec, M. et al.: Understanding desaturation/hydroxylation activity of castor stearoyl D9-Desaturase through rational mutagenesis. *Computational and Structural Biotechnology Journal* **2022**, *20*, 1378-1388.

(27) a) Chalupský, J; Srnec, M.; Yanai, T.: Interpretation of Exchange Interaction through Orbital Entanglement. *J. Phys. Chem. Lett.* **2021**, *12*, 1268–1274. b) Chalupský, J.; Srnec, M.: Beyond the Classical Contributions to Exchange Coupling in Binuclear Transition Metal Complexes. *J. Phys. Chem. A* **2021**, *125*, 11, 2276–2283.

(28) Stein, C. J.; Pantazis, D. A.; Krewald, V.: Orbital Entanglement Analysis of Exchange-Coupled Systems. *J. Phys. Chem. Lett.* **2019**, 10, 6762−6770.

(29) Marenich, A. V.; Ho, J.; Coote, M. L.; Cramer, C. J.; Truhlar, D. G.: Computational electrochemistry: prediction of liquid-phase reduction potentials. *Phys. Chem. Chem. Phys.* **2014**, *16*, 15068-15106.

(30) a) Goldsmith, Z. K.; Harshan, A. K.; Gerken, J. B.; Vörös, M.; Galli, G.; Stahl, S. S.; Hammes-Schiffer, S.: Characterization of NiFe oxyhydroxide electrocatalysts by integrated electronic structure calculations and spectroelectrochemistry. *Proc. Natl. Acad. Sci. U.S.A.* **2017**, *114*, 3050-3055. b) Hammes-Schiffer, S.: Controlling Electrons and Protons through Theory: Molecular Electrocatalysts to Nanoparticles. *Acc. Chem. Res.* **2018**, *51*, 1975-1983.

(31) Yang, X.-H.; Zhuang, Y.-B.; Zhu, J.-X.; Le, J.B.; Cheng, J.: Recent progress on multiscale modeling of electrochemistry. *WIREs Comput. Mol. Sci.* **2021**; e1559.

(32) Sterling, C. M.; Bjornsson, R.: Multistep Explicit Solvation Protocol for Calculation of Redox Potentials. *J. Chem. Theory Comput.* **2019**, *15*, 52-67.

(33) Isegawa, M.; Neese, F.; Pantazis, D. A.: Ionization Energies and Aqueous Redox Potentials of Organic Molecules: Comparison of DFT, Correlated Ab Initio Theory and Pair Natural Orbital Approaches. *J. Chem. Theory Comput.* **2016**, *12*, 2272-2284.

(34) Bím, D.; Rulíšek, L.; Srnec, M.: Accurate Prediction of One-Electron Reduction Potentials in Aqueous Solution by Variable Temperature H-atom Addition/Abstraction Methodology. *J. Phys. Chem. Lett.* **2016**, *7*, 7-13.

(35) Bím, D.; Maldonado-Domínguez M., Rulíšek L., Srnec M. Beoynd the classical thermodynamic contributions to hydrogen atom abstraction reactivity. *Proc. Natl. Acad. Sci. U.S.A.* **2018**, *115*, E10287-E10294.

(36) Mader, E. A.; Larsen, A. S.; Mayer, J. M.: Hydrogen Atom Transfer from Iron(II)−Tris[2,2bi(tetrahydropyrimidine)] to TEMPO: A Negative Enthalpy of Activation Predicted by the Marcus Equation. *J. Am. Chem. Soc.* **2004**, *126*, 8066−8067.

(37) Goetz, M. K.; Anderson, J. S.: Experimental Evidence for pKa-Driven Asynchronicity in C-H Activation by a Terminal Co(III)-Oxo Complex. *J. Am. Chem. Soc.* **2019**, 141, 4051-4062.

(38) Mandal, M.; Elwell, C. E.; Bouchey, C. J.; Zerk, T. J.; Tolman, W. B.; Cramer, C. J.: Mechanisms for Hydrogen-Atom Abstraction by Mononuclear Copper(III) Cores: Hydrogen-Atom Transfer or Concerted Proton-Coupled Electron Transfer? *J. Am. Chem. Soc.* **2019**, *141*, 17236-17244.

(39) Maldonado-Domínguez, M.; Srnec, M.: H-atom Abstraction Reactivity through the Lens of Asynchronicity and Frustration with their Counter-Acting Effects on Barriers. *Inorg. Chem.* **2022**, *61*, 18811–18822.

(40) Maldonado-Domínguez, M.; Bím, D.; Fučík, R.; Čurík, R.; Srnec, M.: Reactive mode composition factor analysis of transition states: the case of coupled electron-proton transfers. *Phys. Chem. Chem. Phys.* **2019**, *21*, 24912-24918.

(41) Maldonado-Domínguez, M.; Srnec, M.: Understanding and Predicting Post H-Atom Abstraction Selectivity through Reactive Mode Composition Factor Analysis. *J. Am. Chem. Soc.* **2020**, *142*, 3947-3958.

(42) Joy, J.; Ess, D. H.: Direct Dynamics Trajectories Demonstrate Dynamic Matching and Nonstatistical Radical Pair Intermediates during Fe-Oxo-Mediated C-H Functionalization Reactions. *J. Am. Chem. Soc.* **2023**, *145*, 7628-7637.

(43) Bharadwaz, P.; Maldonado-Domínguez, M.; Srnec, M.: Bifurcating Reactions: Distribution of Products from Energy Distribution within a Shared Reactive Mode. *Chem. Sci.* **2021**, 12, 12682-12694.

(44) Bharadwaz, P.; Maldonado-Domínguez, M.; Chalupský, J.; Srnec, M.: Reactivity Factors in Catalytic Methanogenesis and their Tuning upon Coenzyme F430 Biosynthesis. *J. Am. Chem. Soc.* **2023**, *145*, 9039–9051.

List of Publications Comprising the Thesis

1. Srnec M., Wong S. D., England J., Que Jr. L., Solomon E. I.: π-Frontier Molecular Orbitals in S=2 Ferryl Species and Elucidation of Their Contributions to Reactivity. Proc. Natl. Acad. Sci. U.S.A. 2012, 109, 14326-14331.
IF: 12.779 **Scopus Citations:** 72

2. Srnec M., Wong S. D., Solomon E. I.: Excited state potential energy surfaces and their interactions in FeIVO active sites. Dalton Trans. 2014, 43, 17567-17577.
IF: 4.569 **Scopus Citations:** 27

3. Srnec M., Iyer S. R., Dassama L. M. K., Park K., Wong S. D., Sutherlin K. D., Yoda Y., Kobayashi Y., Kurokuzu M., Saito M., Seto M., Krebs C., Bollinger Jr J. M., Solomon E. I.: Nuclear Resonance Vibrational Spectroscopy Definition of the Facial Triad FeIV=O Intermediate in Taurine Dioxygenase: Evaluation of Structural Contributions to Hydrogen Atom Abstraction. J. Am. Chem. Soc. 2020, 142, 18886-18896.
IF: 16.383 **Scopus Citations:** 22

4. Wong S. D., Srnec M., Matthews M. L., Liu L. V., Kwak Y., Park K., Bell C. B., Alp E. E., Zhao J., Yoda Y., Kitao S., Seto M., Krebs C., Bollinger Jr. J. M., Solomon E. I.: Elucidation of the Iron(IV)-Oxo Intermediate in the Non-Haem Iron Halogenase SyrB2. Nature 2013, 499, 320-323.
IF: 69.504 **Scopus Citations:** 158

5. Srnec M., Wong S. D., Matthews M. L., Krebs C., Bollinger J. M., Solomon E. I.: Electronic Structure of the Ferryl Intermediate in the α-Ketoglutarate Dependent Non-Heme Iron Halogenase SyrB2: Contributions to H-atom Abstraction Reactivity. J. Am. Chem. Soc. 2016, 138, 5110-5122.
IF: 16.383 **Scopus Citations:** 60

6. Srnec M., Solomon E. I.: Frontier Molecular Orbital Contributions to Chlorination versus Hydroxylation Selectivity in the Non-Heme Iron Halogenase SyrB2. J. Am. Chem. Soc. 2017, 139, 2396-2407.
IF: 16.383 **Scopus Citations:** 104

7. Srnec M., Rokob T. A., Schwarz J., Kwak Y., Rulíšek L., Solomon, E. I.: Structural and Spectroscopic Properties of the Peroxodiferric Intermediate of Ricinus Communis Soluble Δ9 Desaturase. Inorg. Chem. 2012, 51, 2806-2820.
IF: 5.436 **Scopus Citations:** 29

8. Chalupský J, Rokob A. T., Kurashige Y., Yanai T., Solomon E. I., Rulíšek L., Srnec, M.: Reactivity of the Binuclear Non-Heme Iron Active Site of Δ9 Desaturase Studied by Large-Scale Multireference Ab Initio Calculations. J. Am. Chem. Soc. 2014, 136, 15977-15991.
IF: 16.383 **Scopus Citations:** 56

9. Bím D., Chalupský J., Culka M., Solomon E. I., Rulíšek L., Srnec M.: Proton-Electron Transfer to the Active Site Is Essential for the Reaction Mechanism of Soluble Δ9 Desaturase. J. Am. Chem. Soc. 2020, 142, 10412-10423.
IF: 16.383 **Scopus Citations:** 19

10. Chalupský J, Srnec M., Yanai T.: Interpretation of Exchange Interaction through Orbital Entanglement. J. Phys. Chem. Lett. 2021, 12, 1268–1274.
IF: 6.88 **Scopus Citations:** 4

11. Chalupský J., Srnec M.: Beyond the Classical Contributions to Exchange Coupling in Binuclear Transition Metal Complexes. J. Phys. Chem. A 2021, 125, 2276–2283.
IF: 2.944 **Scopus Citations:** 3

12. Bím D., Rulíšek L., Srnec M.: Accurate Prediction of One-Electron Reduction Potentials in Aqueous Solution by Variable Temperature H-atom Addition/Abstraction Methodology. J. Phys. Chem. Lett. 2016, 7, 7-13.
IF: 6.88 **Scopus Citations:** 24

13. Bím D., Maldonado-Domínguez M., Rulíšek L., Srnec M. Beoynd the classical thermodynamic contributions to hydrogen atom abstraction reactivity. Proc. Natl. Acad. Sci. U.S.A. 2018, 115, E10287-E10294.
IF: 12.779 **Scopus Citations:** 58

14. Bím D., Maldonado-Domínguez M., Fučík R., Srnec M.: Dissecting the Temperature Dependence of Electron-Proton Transfer Reactivity. J. Phys. Chem. C 2019, 123, 21422-21428.
IF: 4.117 **Scopus Citations:** 6

15. Maldonado-Domínguez M., Srnec M.: H-atom Abstraction Reactivity through the Lens of Asynchronicity and Frustration with their Counter-Acting Effects on Barriers. Inorg. Chem. 2022, 61, 18811–18822.
IF: 5.436 **Scopus Citations:** 2

16. Maldonado-Domínguez M., Srnec M.: Quantifiable polarity match effect on C-H bond cleavage reactivity and its limits in reaction design. Dalton Trans. 2023, 52, 1399-1412.
IF: 4.569 **Scopus Citations:** 1

17. Maldonado-Domínguez M., Bím, D., Fučík R., Čurík R., Srnec M.: Reactive mode composition factor analysis of transition states: the case of coupled electron-proton transfers. Phys. Chem. Chem. Phys. 2019, 21, 24912-24918. (2019 PCCP HOT Articles)
IF: 3.676 **Scopus Citations:** 9

18. Maldonado-Domínguez M., Srnec M.: Understanding and Predicting Post H-Atom Abstraction Selectivity through Reactive Mode Composition Factor Analysis. J. Am. Chem. Soc. 2020, 142, 3947-3958.
IF: 16.383 **Scopus Citations:** 16

19. Bharadwaz P., Maldonado-Domínguez M., Srnec M.: Bifurcating Reactions: Distribution of Products from Energy Distribution within a Shared Reactive Mode. Chem. Sci. 2021, 12, 12682-12694.
IF: 9.969 **Scopus Citations:** 8

20. Bharadwaz P., Maldonado-Domínguez M., Chalupský J., Srnec M.: Reactivity Factors in Catalytic Methanogenesis and their Tuning upon Coenzyme F430 Biosynthesis. J. Am. Chem. Soc. 2023, 145, 9039–9051.
IF: 16.383 **Scopus Citations:** 0

Bibliometric information from November 2023